# Experimental and numerical analysis of surface nanostructured materials obtained by high energy shot peening

Sara Bagherifard, Ramin Ghelichi
*Politecnico di Milano, Department of Mechanical Eng., Via La Masa 1, 20156, Milano, Italy, sara.bagherifard@mail.polimi.it*

Inès Fernàndez Pariente
*University of Oviedo, Department of Material Science and Metallurgical Eng. Gijón, Spain*

**ABSTRACT.** Surface grain refinement by severe plastic deformation is a relatively new process aimed to enhance mechanical material properties. Among the technological processes used with this aim, shot peening (SP) is one of the most promising, both in terms of costs and as concern the possible production rate. In this study Al7075-T6 bars have been shot peened with parameters (shot speed and treatment duration) much different from those of conventional shot peening. Residual stress state and microstructure gradient have been observed by means of X-ray diffraction (XRD), transmission electron microscopy (TEM), optical microscopy (OM) and nano indentation tester. Formation of a nanostructured layer on top surface of the specimens was confirmed by OM and TEM and also XRD measurements. XRD results show significant depth affected both in terms of residual stress and FWHM. Measurements also indicate of notable improvements in cases of hardness and elastic modulus in comparison with untreated material.
A finite element (FE) model is developed in order to obtain a tool for predicting the effects of treatment parameters on final state of the surface and to interpret the experimental evidence. A detailed approach is chosen for simulating multiple high energy impacts on a 3-dimensional model: the results are in good agreement with experimental evidence.

**KEYWORDS.** Air blast shot peening; Nanostructure; TEM; FEM.

## INTRODUCTION

Great efforts have been recently devoted to produce materials with nanostructured surface and coarse grained underlying layers owing to their highly improved mechanical properties, such as fatigue behaviour [1,2], wear, corrosion and scratch resistance [3,4], hardness [2,5], elastic modulus [3,5], thermal stability [4,6] etc. These processes actually combine superior properties of nanomaterials and conventional engineering materials in order to enhance the performance and service lifetime of the work piece. In fact, since many damage mechanisms (fatigue, pitting, spalling, wear, fretting...) initiate from the surface and propagate to the interior, it is expected that a component with a nanostructured surface layer and coarse-grained interior has highly improved properties. Moreover, the notable compressive residual stresses introduced during the processes utilized to obtain nanostructured surfaces can effectively stop or retard the initiation and propagation of fatigue cracks.
SP is one of the promising methods that have been utilized in this field. It has been reported that particular SP processes can be aimed at achieving ultrafine grained materials on the surface of the treated part [7-12]. These diverse methods which are referred to as surface mechanical attrition treatment (SMAT), ultrasonic shot peening (USSP) and surface nanocrystallization and hardening (SNH), are different from conventional method that is air blast shot peening (ABSP), not only in the needed technological facilities but also for the mechanics of the treatment itself [13].

In this research, Aluminium specimens are treated by ABSP using the conventional SP device and applying an unconventional combination of peening parameters in order to multiply kinetic energy of the process. Results of this parameter modification which is aimed to generate nanograins in the surface layer of the specimen is then investigated in cases of residual stress state using XRD and also microstructure of treated parts using OM and TEM. The unconventional ABSP process is also numerically simulated by means of finite element analyses to provide quantitative description of effects of peening parameters on the surface and to describe the distribution and magnitude of residual stresses and also the thickness of the work-hardened layer. The model developed is also a useful tool to predict the effect of different combinations of peening parameters in the kinetic energy of the process and consequently in the microstructure of the treated part, thus reducing the need of costly experimental work.

## EXPERIMENTAL PROCEDURE

Al7075-T6 bars (Al. alloy 7075) were subjected to two different approaches of air blast shot peening using unlike combinations of parameters as shown in Tab. 1, both of which are considerably different from traditional parameters used for this material.

| Specimen label | Shot diameter [mm] | Air speed [m/s] | Almen Intensity [0.0001 inch] | Treatment time [s] |
|---|---|---|---|---|
| A | 0.6 | 90 | 7C | 450 |
| B | 0.6 | 90 | 7C | 900 |

Table1: Aspects of the SP processes.

To study the state of residual stresses, XRD analysis of surface layer in the as-treated specimens was performed using an AST X-Stress 3000 X-ray diffractometer (radiation Cr Kα, irradiated area 1mm², $\sin^2\psi$ method, diffraction angles (2θ) scanned between -45 and 45). To study the trend of residual stresses, measurements were carried out in depth step by step removing a very thin layer of material using an electro-polishing device. Grain size measurements were performed by another in situ high-energy synchrotron X-ray diffraction device to obtain grain size and also microstrain distribution.
Microstructure of the surface layer was observed by TEM using a Philips CM12 microscope operating at 120 kV. To perform TEM observations very thin pieces of specimens were first cut by electrical discharge machine (EDM) then were mechanically polished from the untreated side and finally the last step of thinning was performed by means of ion milling with proper incident angles. Hardness and elastic modulus were measured on treated surface using nano Indentation tester (NHT).
Microstructure observations were carried out also through OM. For these observations the specimens were etched by Keller's reagent.

## NUMERICAL SIMULATION

### *Geometry/FE model and material properties*

A three-dimensional geometry model as shown in Fig. 1 is developed using commercial finite element code ABAQUS/Explicit 6.7. The specimen is modelled as a rectangular body chosen sufficiently large to avoid boundary effects, with the impact area of (0.1*0.1 mm²) considered in the central part. Specimen mesh is set up by 8-node linear brick elements with reduced integration and hourglass control (C3D8R). All side faces including target's base are surrounded by so-called half infinite elements that provide quiet boundaries by minimizing the reflection of dilatational and shear waves back in to the region of interest and preventing them from affecting the state of stress of the model when static equilibrium is reached. Infinite elements are allowed only linear with elastic behaviour so they must be positioned at a sufficient distance from the non-linear interaction region to ensure accuracy [14]. Combined isotropic and kinematic material is used to describe target material's behaviour.
Steel shots with a diameter of 0.6 mm similar to the shots used in experiment are modelled as half spherical bodies consisting of tetrahedral elements (C3D4) with an isotropic elastic behaviour and a density twice the real density of steel

to make up for modelling half of the shot. Velocity in the z-direction is defined as initial condition to all the shots, regarding an impact angle=90º as it is typical for ABSP.
General contact is used as the criteria of the contact between shots and target surface with an isotropic Coulomb friction coefficient equal to $\mu$= 0.2.

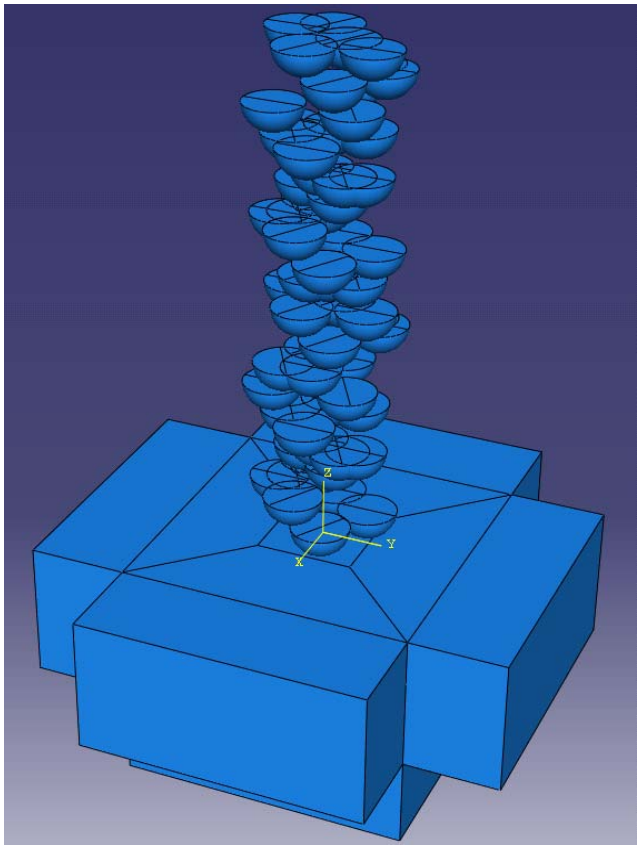


Figure 1: 3D model used for multiple impact simulation

*Mesh convergence*

In all studies performed on numerical simulations of shot peening, fine mesh has been used in the impact area and coarser elements in the area far from impact region. While the size of elements utilized in these simulations are so diverse and there are not so many references providing justifications about their element size choice. Besides all the few mesh convergence studies have focused on obtaining a good resolution of the residual stress distribution under impact area. Frija et al. carried out a sensitivity study to optimize dimensions of the elements in refined zone, by comparison with the elastic Hertz contact problem [15]. Zimmerman et al used an element size equal to $1/15^{th}$ of the dimple diameter produced by a single shot impact for the modelled shot diameter and velocity for which convergence was obtained in terms of stresses [16]. Klemenz et al. also used Hertz analytical solution for a purely elastic material behaviour to examine the accuracy of FE mesh in the cases of single and double impact model and for multiple impacts they chose the size of elements equal to $1/10^{th}$ of dimple size [17].
In this study the effect of element size not only on stress state but also on the strains particularly in terms of equivalent plastic strain (PEEQ) is examined since PEEQ is the parameter that has a key role in coverage estimation. A single impact was simulated in order to estimate the dimensions of plastic indentation generated on target surface by a single shot impact. Then convergence evaluation was performed changing element size in impact zone of the target as a ratio of this dimple diameter. The results indicate that with very fine mesh convergence can be reached earlier in terms of residual stresses in the impact zone than in the case of PEEQ.
Another interesting observation is that considerable changes were monitored with changing size of shot elements. This is the issue that has not been regarded in any of the shot peening simulations available in literature since all the few studies have been performed on the basis of target element size. In fact most of researchers have chosen rigid elements for the numerical simulations [18, 19-21] and in those who regarded deformable shots there is no validation for element size on

shots. Another common point in all simulations is that size of shot element has always been regarded much coarser that the size of elements in the impact region [15, 22-24]. In this series of studies for mesh convergence due to computational costs the size of element on the shots was chosen as $1/10^{th}$ of dimple diameter in multiple impact simulation. And the size of elements on impact zone was fixed at $1/20^{th}$ of dimple diameter. These choices result in satisfying convergence in terms of stress and also PEEQ in impact zone. Close view of mesh density in impact zone is shown in Fig.2.

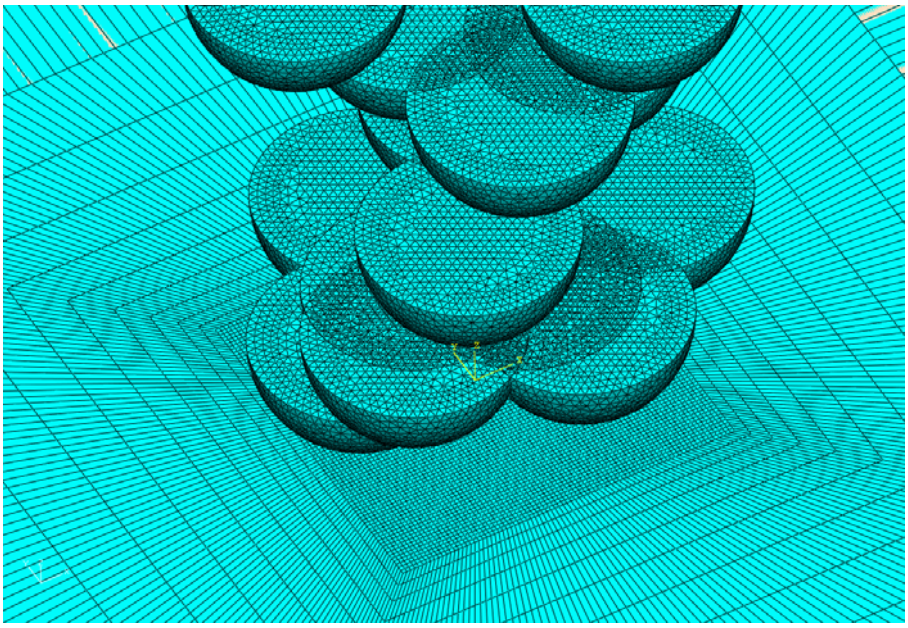

Figure 2: Close view of elements in impact zone.

*Coverage assessment*

To achieve a realistic modelling of SP process the developed finite element model shall consist of a large number of identical shots impinging the target with an impact angle of 90° at random locations and in random sequences.

Surface coverage defined as the ratio of the area covered by plastic indentation to the whole surface area treated by shot peening is one of the most important input variables in SP simulation. Specifying a required level of coverage is a necessary starting point. However no comprehensive investigations have been carried out yet on how to model coverage accurately [25].

In order to predict and control coverage an efficient quantitative procedure shall be applied at several locations. All theoretical and practical evidence point to an exponential approach to 100% coverage as the amount of peening is increased [26]. The established relationship between coverage (C) and the ratio of total indent area to the target area ($A_r$) is given in Eq.1:

$$C\% = 100\left[1 - e^{-Ar}\right] \quad (1)$$

A realistic target for coverage is set which defines full coverage as being equivalent to 98% actual coverage. According to Equation.1 full coverage is achieved when an indent ratio of 4 is reached. In our case regarding dimensions of target surface and single impact indentation area, we will need 67 impacts to obtain full coverage.

In order to obtain a realistic simulation, the impact sequence and arrangement of these 67 shots was generated arbitrarily by using a Random function. It is shown in [24] that shot impacts one after the other has a different influence on the development of residual stresses with respect to impacting simultaneously. Due to this phenomenon many researchers have avoided simultaneous impacts. Nevertheless since simultaneous impact is a very frequent event in practical shot peening it was not avoided in this simulation taking in to account that it would be also helpful to decrease computational costs.

Impact sequence which provides a dimple pattern of full coverage on the surface is shown in Fig. 3. The random sequence has been arranged in a way to cover a circular region with an area equal to area covered by X-ray radiation during XRD measurements in order to obtain comparable results with experimental measurements. The arrangement is repeated so as to simulate 67 shot impacts to the target surface.

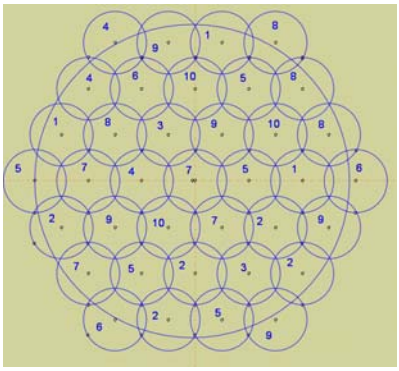

Figure 3: Arrangement and order of impacts representing the area over which residual stress measurements was performed.

## RESULTS AND DISCUSSION

### *OM observations*

As illustrated in Fig. 4, from the overall observation of the cross sections in optical microscope, a distinct region separated with sharp boundaries from the underlying layer is easily recognized on the top surface of specimens A and B. The underlying layer is the work hardened layer which is strongly deformed. The uniform contrast layer near the surface as stated by Saitoh et. al is considered to be the fine grained layer which changed the colour after etching. It is reported that the repeatedly folding of the deformed regions leads to the formation of such fine grained regions at the surface of the specimens [27].

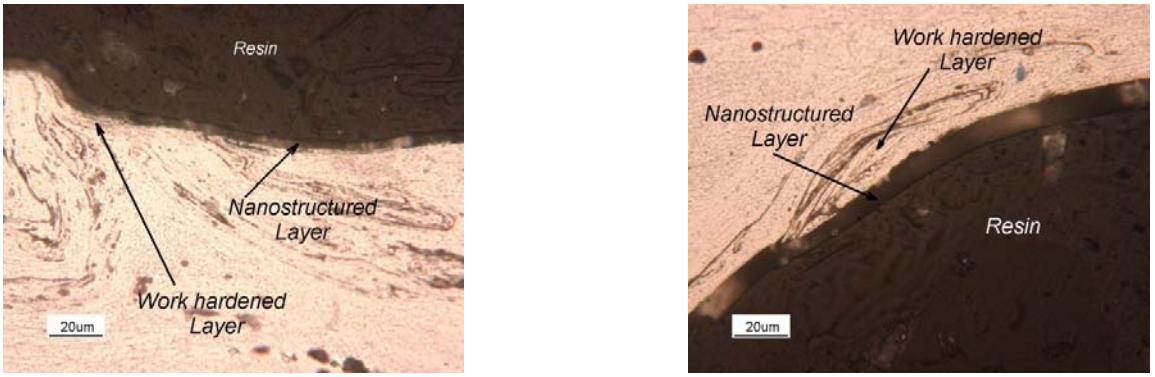


(a) (b)

Figure 4: Cross-sectional optical microscopic images of the two samples (500X). a) specimen A; b)specimen B

The nanostructured layer does not have a constant and regular thickness around the section observed by microscopy however it seems that increasing treatment time has leaded to rise in the nanostructured layer thickness. The average thickness of nanostructured layer for specimen A is about 6 μm while for specimen B is measured to be around 11 μm.
The grain refinement process can be enlightened with this description that the unconventional SP process provides repeated multidirectional mechanical loads with high kinetic energy onto the material surface. The peening loads generate dislocations and eventually result in plastic deformation in the surface layer of the material. Repeated shot peening with high energy creates more dislocations which may be annihilated or recombined (rearranged) to form small angle grain boundaries separating individual grains, as proposed by Fecht in analyzing the grain refinement of metals during ball milling [28].

### *Analysis of residual stress profile obtained from XRD and FEM*

Stresses measured by X-ray diffraction are usually an average value of the stresses in the area covered by X-ray. To compare multiple impact simulation results with the XRD measurements a method suggested by Schwarzer was used [24].

In this method average of residual stresses in an area equal to the one affected by X-ray was calculated at each depth. The chosen area in the finite element model is a circle fit in the impact zone. Within this area an average of the stress components at the Gauss points of adjacent elements parallel to the surface is calculated for each element layer in order to simulate the residual stress profile also after layer removal where the residual stresses were determined at the new surface. The obtained results are compared with XRD measurements in Fig.5. Experimental results imply that a considerable depth of material is characterized with significant compressive residual stresses in both specimens. FEM results have acceptable consistence with XRD measurements.
The most notable difference is observed for values over the specimen's surface taking in to consideration that in case of FEM results, the fist presented value is not over the surface but at the depth of 0.06 mm where is the position of integration points of first element's layer. This difference can be related to the significant roughness over the surface of specimens due to high energy shot peening. The high points in the rough surface contribute more to the diffraction pattern and consequently they introduce some errors to the XRD measurements on the first layers [29]. In Fig.5 it is also possible to note that increasing treatment time has produced very slight difference in the results. It can be concluded that changing process time in this scale is not notably affecting state of residual stresses.

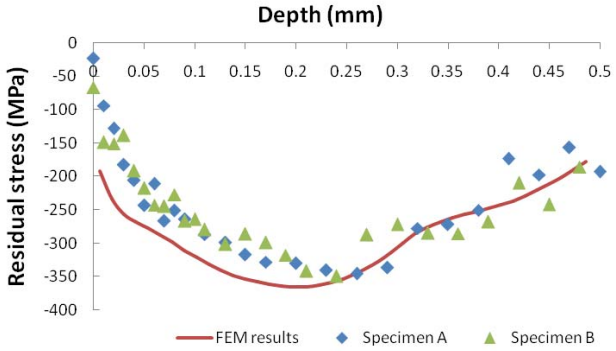


Figure 5: Distribution of macroscopic residual stresses obtained by XRD and FEM as a function of position measured from impacted surface.

## *FWHM measurements by XRD*

Another parameter measured by X-ray diffraction, FWHM, that is the width of the diffraction peak at half the maximum diffraction, is shown in Fig. 6. It is measured as an index of hardening of material, and of the crystal size. As shown in Fig. 6 maximum FWHM is observed on the surface of specimen, declining down to the depth. Also in terms of FWHM in the surface region there is no considerable difference between the results for specimen A and B but getting farther from impacted surface FWHM values decrease more rapidly in specimen A. It seems that the thickness of work hardened layer is more pronounced in specimen B and this can be attributed to increasing process time.
Fig. 7 shows the effective plastic strain as a function of the location measured from the impacted surface obtained by the FE analysis, calculated with the same averaging method employed for stresses.
It is interesting to note that the thickness of the work-hardened layer obtained from FEM is nearly the same as the depth which shows considerable FWHM values (Fig. 6), really similar to the thickness of layer with notable residual compressive stresses (Fig. 5).

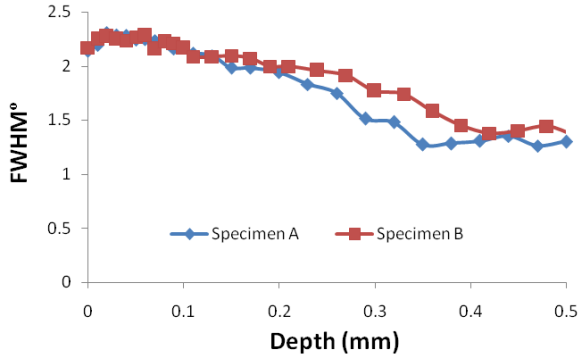


Figure 6: FWHM profile obtained by XRD as a function of position measured from impacted surface.

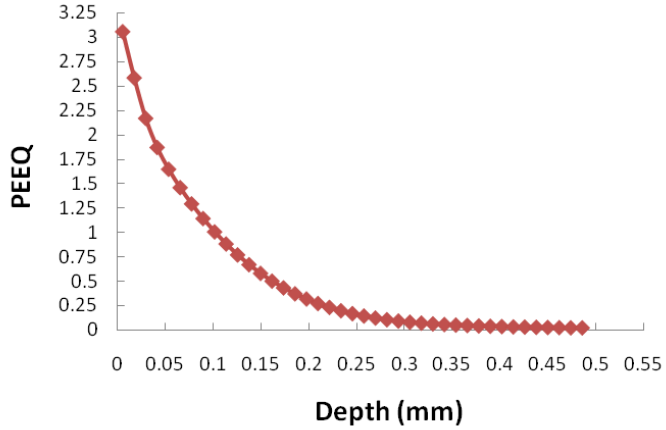


Figure 7: Effective plastic strain profile within the target measured from impacted surface obtained by FE analysis.

### *Grain size measurements by XRD*

Fig. 8 presents X-ray diffraction patterns of specimen B. XRD analyses were carried out for determining average grain size and microstrain in the surface layer. Diffraction peaks of a Si internal standard sample were used as a reference, to represent the instrumental broadening. The experimental data were analyzed via MAUD program (Materials Analysis Using Diffraction) [30], through Rietveld procedure using isotropic size-strain model [31]. The Rietveld method uses multiple reflections of experimental data and can determine structural and microstructural parameters (lattice parameters, atomic coordinates, thermal factors, crystallite size, microstrain and so on).

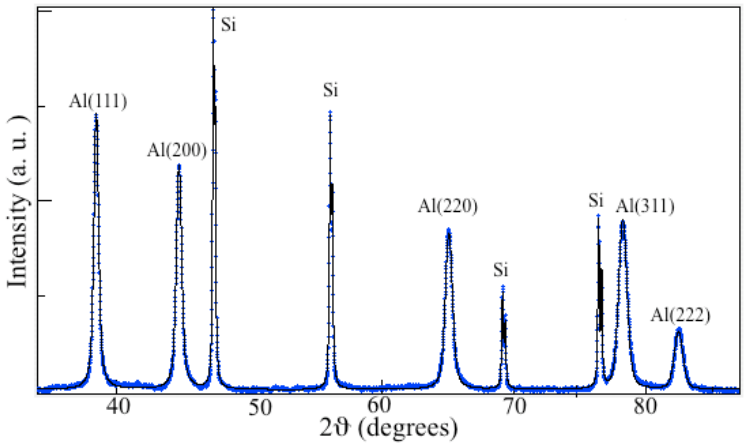


Figure 8: X-ray diffraction patterns of the specimen B.

For the top surface layer, evident broadening of Bragg diffraction peaks was seen owing to a grain refinement and increase in the atomic-level microstrain. The average grain size was found to be about 56 nm for specimen A and 53 for specimen B. Measured mean microstrain was 0.00208 (*r.m.s.*) and 0.00233 (*r.m.s.*) for specimen A and B respectively. Results indicate that grain size and internal strain introduced by this method of SP does not change remarkably with the processing time.

### *TEM observations*

Fig. 9 shows TEM bright-field image and the corresponding selected area diffraction (SAD) pattern obtained at impacted surface of specimen A. The bright field image (Fig. 9.a) represents irregularly shaped grains the average size of which is measured to be 50 nm. This mean size is close to the average grain size obtained from XRD measurement.
SAD pattern (Fig. 9.b) is composed of partially continuous diffraction rings, which confirm that the as-received large crystalline grains have been broken down to nanograins at this region. Theses diffraction patterns also clearly indicate that nanograins at impacted surface have completely random orientations with high-angle grain boundaries. Based on TEM observations, it can be observed that the nanostructured layer has a grain-size gradient as the locations moves from the impacted surface.

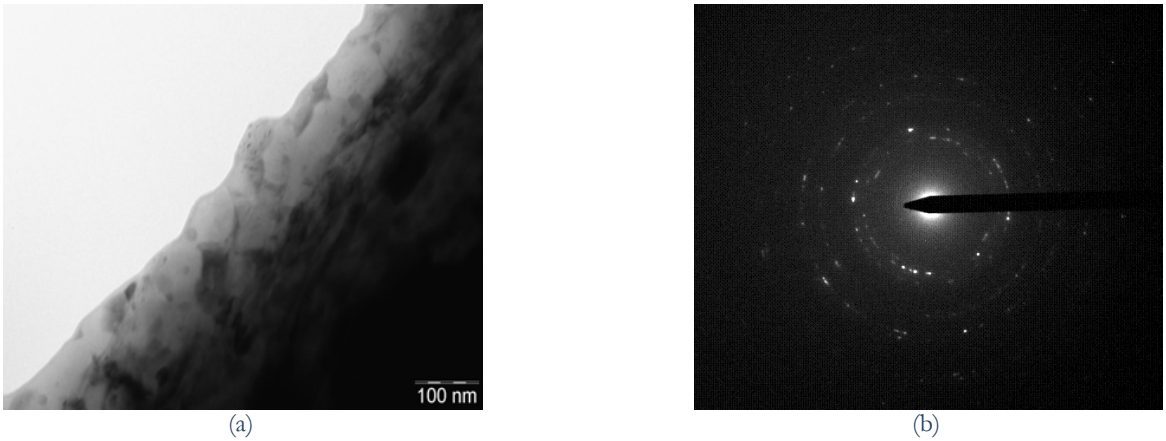


(a) (b)

Figure 9: Plane-view TEM observations and grain size distributions of specimen A
a) bright-filed image of the impacted surface showing the formation of nanograins b) correspondent SAD pattern

*Nanohardness and elastic modulus measurement*

Hardness and elastic modulus were measured on specimens surface using NHT device which is a machine especially suited to perform measurements on films with thickness in micrometer or lower scale. Various indentation matrixes have been performed on shot peened surface of each specimen. The mean results of these measurements are listed in Tab. 2.

| | Vickers hardness [HV] | Elastic Modulus [GPa] |
|---|---|---|
| Specimen A | 210 | 100 |
| Specimen B | 240 | 106 |
| Typical values of Al7075-T6 [32] | 175 | 70 |

Table 2. Vickers hardness and elastic modulus for specimens A and B

As shown in Table.2 this unconventional SP process has lead to improvements up to 20% and 37% in hardness of specimens A and B respectively and also an enhancement of 30% in elastic modulus for both specimens. Comparing the results obtained for specimen A and B, it is approved that increasing SP time has lead to increment of hardness but no notable change is seen in terms of elastic modulus.

## CONCLUSIONS

Properties of Al7075 bars treated by unconventional method of ABSP have been investigated by XRD measurements, OM, TEM observations and nanohardness tester.

Microscopic observations and XRD results confirm that using high kinetic energy shot peening has lead to creation of a nano grained layer on surface of the specimens. The nanocrystallized layer shows improved hardness and modulus of elasticity. Trend of FWHM seems to follow the structure gradient from fine grained surface layer to coarse-grained bulk material. Among the parameters selected to increase kinetic energy of the shots, treatment time seems to be less efficient in altering residual stresses in the top surface layer while they have notably increased thickness of nanostructured layer.

Finite element analysis was also performed to simulate the high energy shot peening process. Developing a model to analyze the process of high energy shot peening is useful for optimization of the peening processes and also for predicting material state after peening without having to conduct costly experiments. Experimental results of XRD measurements were in good agreement with the results obtained from numerical simulation.

Overall the employed unconventional SP process appears to be a promising method to produce advanced materials for strength-intensive service applications showing especially remarkable improvement in fatigue and fracture behaviour which are greatly sensitive to grain size.

## ACKNOWLEDGEMENT

We would like to thank Ing. Michele Bandini for his contribution to this research and execution of shot peening in Peen Service srl.

## REFERENCES

[1] X.P. Jiang, X.Y. Wang, J.X. Li, D.Y. Li, C.S. Manc, M.J. Shepard, T. Zhai, Material Science and Engineering A, 429 (2006) 30.
[2] J.W. Tian, J.C. Villegas, W. Yuan, D. Fielden, L. Shaw, P.K. Liaw, D.L. Klarstrom, Materials Science and Engineering A, 468–470 (2007) 164.
[3] L. Wang, D.Y. Li, Surface and coating technology, 167 (2003) 188.
[4] W.P. Tong, C.Z. Liu, W. Wang, N.R. Tao, Z.B. Wang, L. Zuoa and J.C. He, Scripta Materialia, 57 (2007) 533.
[5] L. Huang, J. Lu, M. Troyon, Nanomechanical, Surface & Coatings Technology, 201(2006) 208.
[6] J.L. Liu, M. Umemoto, Y. Todaka, K. Tsuchiya, Materials science, 42 (2007) 7716.
[7] N.R.Tao, M.L.Sui, J.Lu, K. Lua, Nanostructured Materials, 11 (1999) 433.
[8] G. Liu, J. Lu, K. Lu, Materials Science and Engineering A, 286 (2000) 91-95.
[9] X. Wu, N. Tao, Y. Hong, B. Xu, J. Lu, K. Lu, Acta Materialia, 50 (2002) 2075.
[10] Z.G. Liu, H.J. Fecht, M. Umemoto, Materials Science and Engineering A, 375–377 (2004) 839.
[11] Y. Todaka, M. Umemoto, K. Tsuchiya, Materials Transactions, 45 (2004) 376.
[12] F.A. Guo, N. Trannoy, J. Lu, Materials Science and Engineering A, 369 (2004) 36.
[13] S. Bagheri Fard, M. Guagliano, Surface Engineering, 25(1) (2009) 3.
[14] ABAQUS Analysis User's Manual (2007), version 6.7, infinite elements, Section 22.2.1
[15] M.firja, T. Hassine, R.Fathallah, C.Bouraoui, A.Dogui, Material Science and Engineering A, 426 (2006) 173.
[16] M. Zimmerman, V. Schulze, H.U. Baron, D. Lohe, Proceeding of the 10th International Conference on Shot Peening (ICSP10), Tokyo Japan (2008) 63.
[17] M. Klemenz, V.Schulze, O.Vohringer, D.Lohe, Material Science Forum, 524-525 (2006) 349.
[18] Al-Hassani S.T.S, Proceedings ICSP-7, Warsaw Poland (1999) 217.
[19] T. Hong, J.Y. Ooi, J. Favier, B. Shaw, Proceedings ICSP-9, Paris France (2005) 34.
[20] M. Guagliano, L. Vergani, M. Bandini, F. Gili, Proceedings ICSP-7, Warsaw Poland (1999) 274.
[21] S.A. Meguid, G. Shagal, J.C. Stranart, J. Daly, Finite Elements in Analysis and Design 31 (1999) 179.
[22] G.H.Majzoobi, R. Azizi, A. Alavinia, J. of Material Processing Technology, (2005) 1226.
[23] S.A. Meguid, G,Shagal, J.C. Stranart, Int. J. of Impact Engineering, 27 (2002) 134.
[24] J. Schwarzer, V. Schulze, O. Vohringer, Proceedings from International Conference of Shot Peening (ICSP8), Munich Germany (2002) 507.
[25] V. Schulze, M. Klemenz, M. Zimmerman, Proceedings of the 10th International Conference on Shot Peening (ICSP10), Tokyo Japan (2008) 53.
[26] D.Kirk, The Shot Peener, 23-2 (2009) 24.
[27] H.Saitoh, T.Ochi and M.Kubota, Proceedings of the 10th International Conference On Shot Peening, Tokyo Japan (2008) 488.
[28] H. J. Fecht, Nanophase Materials, ed. G. C. Hadjipanayis and R. W. Siegel, Kluwer Academic Publishers, Dordrecht, the Netherlands (1994).
[29]B.D.Cullity, S.R.Stock, Elements of X-ray diffraction, Prentice Hall Inc (2001).
[30] L. Lutterotti,S. Matthies, H.R. Wenk, A.S. Schultz, J.W. Richardson, J. of Applied Physics, 81 (1997) 594.
[31] H.M. Rietveld, J. of Applied Crystallography, 2 (1969) 65.
[32] ASM Handbook, Fatigue and Fracture, Materials Information Society, Materials Park OH 19-1st ed. (1996).